MINISTERUL EDUCAȚIEI NAȚIONALE
ROMÂNIA
UNIVERSITATEA DE MEDICINĂ, FARMACIE, ȘTIINȚE ȘI TEHNOLOGIE „GEORGE EMIL PALADE" DIN TÂRGU MUREȘ

Acta Marisiensis. Seria Technologica
Vol. 20 (XXXIV) no. 2, 2023
ISSN 2668-4217, ISSN-L 2668-4217

sciendo

10.2478/amset-2023-0010

OBTAINING AND CHARACTERIZING THE DIELECTRIC AND FERROELECTRIC PROPERTIES OF THE PZT-PMS COMPLEX SYSTEM THROUGH SOLID STATE REACTIONS AND SPARK PLASMA SINTERING

Alina Iulia DUMITRU[1,a], Dorinel TALPEANU[2], Rodica Mariana ION[3,a], Ildiko PETER[4*]

[1,2]National Institute for Research & Development in Electrical Engineering ICPE-CA, 313 Splaiul Unirii, 030138, Bucharest, Romania
[a]Valahia University from Targoviste, Doctoral School of Materials Engineering, Targoviste, Romania
[1]alina.dumitru@icpe-ca.ro, [2]dorinel.talpeanu@icpe-ca.ro,
[3] National Institute for Research and Development in Chemistry and Petrochemistry – ICECHIM, 202 Splaiul Independentei, 060021, Bucharest, Romania
[3]rodica_ion2000@yahoo.co.uk,
[4]„George Emil Palade" University of Medicine, Pharmacy, Science and Technology of Targu Mures, Nicolae Iorga no. 1, 540139, Targu-Mures, Romania
ildiko.peter@umfst.ro

Abstract

In this paper B-oxide sintering process and Spark plasma Sintering (SPS) method is used to synthesize $0.88Pb(Zr_{0.52}Ti_{0.48})O_3 - 0.12Pb(Mn_{1/3}Sb_{2/3})O_3$ – x at%Pr complex system where x = 0 and 0.02. The sintering temperature used in the SPS technique is considerably lower than that used in the B-oxide method (200 to 400°C) with significant decrease of the duration of the sintering route, arriving to some minutes instead of some hours.
The aim of the study is the investigation of the effect of sintering technique on the dielectric and ferroelectric properties of such piezoelectric materials. The properties of the developed ceramic materials were determined: the development of crystalline phases was investigated by X-ray diffraction technique and the microstructural behavior by scanning electron microscopy was observed. The composition obtained by the SPS technique shows a lower remnant polarization and maximum strain, as well as a higher coercive field, compared to the those obtained using the same composition produced by B-oxide method.

Key words: PZT compositions; SPS technique; high density; perovskite structure; electrical properties

1. Introduction

Lead zirconate titanate (PZT) based piezoelectric materials, named "intelligent materials", are used in "smart" applications for sensing and actuating purposes. These "intelligent materials" are employed as sensors and actuators [1]. For piezoelectric materials, there is an interdependence between the composition, the structure and the electrical properties obtained [2,3]. The values obtained for the properties of the piezoelectric materials is governed by the sintering method used. The values obtained for the physical and electrical properties depend on the method of obtaining these materials. The most often used procedures used for the development of intelligent materials are conventional mixed oxides technique [4,5], B-oxides technique [6], two-step columbite method [7], sintering by hot pressing [8]

and a relatively new technique spark plasma sintering (SPS) [9], etc. Compositions from complex systems based on lead titanate-zirconate solid solutions are conventionally sintered at high temperatures (higher than 1150°C) for more than 1 hour. At these high temperatures, the atmosphere has to be saturated with lead oxide (PbO) during sintering, because at temperatures higher than 950°C the volatilization of PbO increases. Evaporation of lead (Pb) leads to compositional fluctuations in the case of sintering of PZT-based materials and implicitly affects the piezoelectric and dielectric properties, decreasing them [10]. On the other hand, it is quite difficult to control the compositional fluctuation of the complex compositions obtained by the conventional sintering method [11]. The main advantages of the spark plasma sintering method (SPS) compared to the conventional sintering methods (hot pressing (HP), hot isostatic pressing (HIP) and sintering in furnaces with atmosphere) are the low sintering temperature and the very short time of the sintering process [12].

The materials obtained by SPS technology exhibit relatively high values for dielectric, ferroelectric and piezoelectric properties [13,14].

In the present paper the PZT complex systems with the composition **$0.88Pb(Zr_{0.52}Ti_{0.48})O_3 - 0.12Pb(Mn_{1/3}Sb_{2/3})O_3$ – x at% Pr** (x= 0; 2) were obtained by SPS technology and by using conventional technology. The calcined powders used in the mentioned processes were obtained using the B-oxide method. The microstructure and electrical properties were comparatively investigated.

2. Materials and Methods

In the present paper $0.88Pb(Zr_{0.52}Ti_{0.48})O_3 - 0.12Pb(Mn_{1/3}Sb_{2/3})O_3$ – x at% Pr (with x = 0; 2) complex compositions were synthesized by sintering using two technological variants (i) the conventional sintering method (in furnace, in air) and (ii) SPS technology. The compositions were labelled as (i) CS-MP, CS-MPPr and (ii) SPS-MP, SPS-MPPr respectively. To obtain the complex compositions powders for sintering, the B-oxide precursor method was used. The conventional method consists in obtaining the $MnSb_2O_6$ powder in a first stage. The $MnSb_2O_6$ powder thus obtained is further used as a raw material together with the other constituent oxides. $MnSb_2O_6$ powder was obtained by sintering (at 1000°C, 10 hours) a stoichiometric mixture of pure Sb_2O_5 (>99%) and pure $MnCO_3$ (>99%), and then finely milled in distilled water for 10 hours and dried at 80°C. Chemical composition and phase purity of $MnSb_2O_6$ powder were determined using X-ray diffraction. In the second step the $MnSb_2O_6$ powder obtained in the first stage together with high purity (>99%) oxides powders PbO (Merck), ZrO_2 (Merck), TiO_2 (Aldrich), Pr_2O_3 (Aldrich) were used as raw materials. The powders were mixed as per stoichiometric ratios and ball milled for 10 hours using agate balls and water as liquid media. After milling, the powders were dried and calcined at 840°C for 4 hours in closed alumina crucibles. In alumina crucibles as a protective medium was used $PbZrO_3$ powder to prevent evaporation of the PbO. The calcined powders were milled again (for 10 hours) in distilled water, dried and sieved. The powders consequently obtained were sintered in a graphite die, in the form of disks (with 20 mm in diameter), by using the SPS equipment in vacuum, under a pressure of 50 MPa. In SPS the powders (6g/sample) were sintered at two different temperatures (850°C and 950°C) for 5 minutes using a rate of increasing the temperature of 50°C /min (controlled by the applied current). To avoid the carbon contamination of the samples boron nitride spray is employed.

For comparison, the calcined powders were granulated (with PVA aqueous solution 5%), uniaxially pressed in the form of discs (with 20 mm in diameter) and then sintered at 1150 and 1250°C, in air for 2 hours using a Carbolite type furnace.

After SPS sintering and normal sintering in furnace, the samples were polished on both sides and covered with Ag paste to obtain electrodes for electrical measurements. Densities of the sintered samples were measured by Archimedes method. The crystalline structure of the sintered samples was determined by X-ray (XRD) diffraction using BRUKER AXS D8 Advance diffractometer with CuKα radiation and Ni filter. The microstructure was determined using scanning electron microscope (FESEM-FIB Workstation Auriga produced by Carl Zeiss, Germany). The dielectric properties were measured at 1kHz using LCR meter HM 8018 (HAMEG type). The ferroelectric properties (P-E hysteresis loops) were determined using the TF analyser 2000 (Aixact System) and the piezoelectric properties were measured using an impedance analyzer 4294A (Agilent type). The resonance-antiresonance method was used to determine the electromechanical coupling factor k_p.

3. Results and discussion

XRD investigations

Fig.1 shows the XRD diffraction spectrum obtained for the precursor powder calcined for 10 hours at 1000°C. The specific lines of the $MnSb_2O_6$ compound

were identified. Rietveld analysis was used to determine the obtained lattice parameters. The crystallite size obtained was 62.6 nm along with the lattice parameters values: a (Å) = 8.7977 and c (Å) = 4.7216 [15].
Fig.2-5 shows the XRD diffraction spectra for all the sintered piezometerials. Fig.2 and Fig.3 shows the XRD diffraction spectra for MC-MP and MC-MPPr piezo materials sintered at 1150°C and 1250°C for 2 hours.

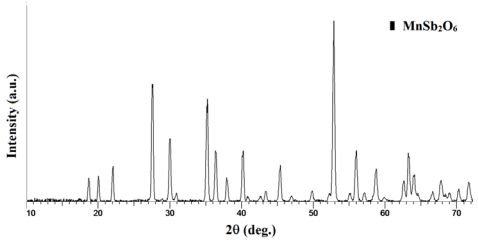

Fig.1 XRD diffraction spectrum obtained for the precursor powder

Fig.4 and Fig.5 shows the XRD diffraction spectra for SPS-MP, SPS-MPPr sintered at 850°C and 950°C for five minutes. For the compositions obtained by the conventional sintering method diffraction spectra indicate the formation of lead zirconate titanate solid solution $Pb(Zr_{0.52}Ti_{0.48})O_3$ (with tetragonal structure) as the majority phase and a secondary pyrochlore phase $Pb_2(ZrSb)O_{6,5}$ [16] (Fig.2, Fig.3). The pyrochlore phase appears as a result of the decomposition of a part of the perovskite phase because of the lead volatilization during sintering at high temperatures [17].

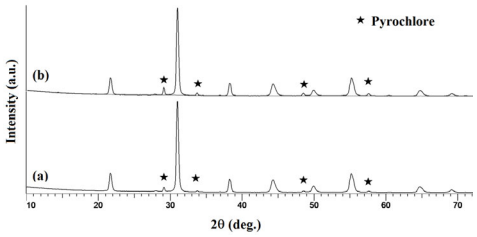

Fig.2 XRD diffraction spectra of (a)MC-MP and (b)MC-MPPr sintered at 1150°C for 2h

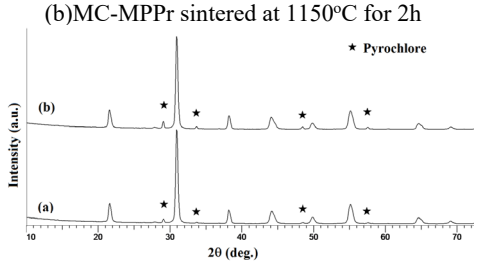

Fig.3 XRD diffraction spectra of (a)MC-MP and (b)MC-MPPr sintered at 1250°C for 2h

The intensity of the diffraction peaks belonging to the majority phase increase in intensity with the increase of the sintering temperature from 1150°C to 1250°C. The level of tetragonality (identified by the c/a ratio) of the crystal lattice varies with the sintering temperature and is directly influenced by the nature and amount of the phases developed. When the sintering temperature increases from 1150°C to 1250°C, the values obtained (Table 1) for the ratio c/a increase too [18, 19]. As we presented in a previous work, heterovalent ions such as Pr^{3+} act as "softener" donor, doping the perovskite structure at the A^{2+} positions replacing Pb^{2+} and obtaining lead vacancies (V_A^{2-}) for compensation [20].
The formation of (V_A^{2-}) is expected to increase the remanent polarization with the homogeneous decrease of the lattice strain [20].

Table 1:Teragonality (c/a ratio) and lattice parameters of MC-MP and MC-MPPr as function of sintering temperature

Temperature [°C]	Lattice parameters	MC-MP	MC-MPPr
1150	**c [Å]**	4.094	4.092
	a [Å]	4.061	4.058
	c/a	1.0081	1.0083
1250	**c [Å]**	4.096	4.095
	a [Å]	4.095	4.057
	c/a	1.0089	1.0093

For the compositions obtained by SPS method (Fig.4 and Fig.5) diffraction spectra indicate, also, the development of lead zirconate titanate solid solution $Pb(Zr_{0.52}Ti_{0.48})O_3$ as the majority phase. The position of the peaks in the XRD diffraction spectra obtained by the SPS method have the same angular position. The differences that appear compared to the modified conventional method are related to the type of secondary phases. The secondary phases were identified as oxides.

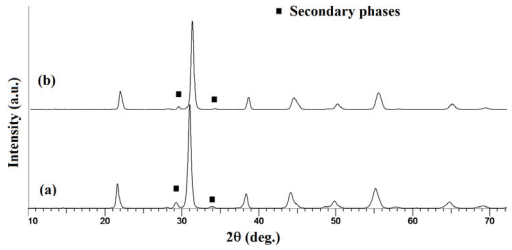

Fig.4 XRD diffraction spectra of (a)SPS-MP and (b)SPS-MPPr sintered at 850°C for 5'

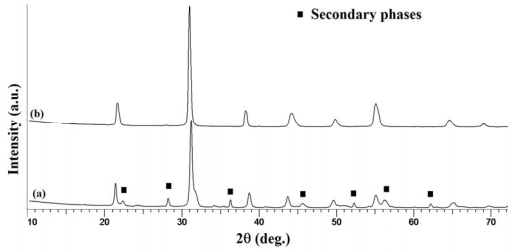

Fig.5 XRD diffraction spectra of (a)SPS-MP and (b)SPS-MPPr sintered at 950ºC for 5'

Table 2: Teragonality (c/a ratio) and lattice parameters of SPS-MP and SPS-MPPr as function of temperature

Temperature [ºC]	Lattice parameters	SPS-MP	SPS-MPPr
850	**c [Å]**	4.094	4.096
	a [Å]	4.051	4.053
	c/a	1.0106	1.0106
950	**c [Å]**	4.131	4.098
	a [Å]	3.971	4.056
	c/a	1.0403	1.0103

The values obtained for the tetragonality of the crystal lattice (ratio c/a) (Table 2) increase with the increase of the SPS sintering temperature from 850ºC to 950ºC and are higher than in the case of the conventional sintering method [21].

Sinterability

Table 3 shows the obtained densities of the MC-MP, MC-MPPr, SPS-MP and SPS-MPPr piezo materials. For all the compositions, the values obtained for the apparent density increase with the increase of the sintering temperature.

The comparison of the values obtained for the relative densities to its' theoretical value (of 8.002 g/cm^3) [22], indicates values higher than 95%. At this point one can assume that all compositions synthesized are practically at full density.

Table 3: Piezo materials density as a function of sintering temperature

Samples	Temperature [ºC]	Apparent density [g/cm^3]
MC-MP	1150	7.69
	1250	7.83
MC-MPPr	1150	7.71
	1250	7.85
SPS-MP	850	7.82
	950	7.91
SPS-MPPr	850	7.85
	950	7.95

The values obtained in the case of sintering by the SPS method are higher than the values obtained in the conventional sintering process, being in accordance with the data from the literature [17].

Microstructure

In the Fig.6 are reported the SEM images of the piezo materials sintered for 2 hours at 1150ºC and 1250ºC. The high-resolution SEM images show a microstructure made up of 2 types of grains. The high-resolution SEM images (x20.00kX) exhibit a microstructure made up of 2 types of polyhedral grains, one of micrometer size and one of submicron size. The small grains are well faceted. The size of the grains depends on the sintering temperature and the composition [23]. The sizes of small granules increase with increasing temperature, while the sizes of large granules decrease with increasing temperature. Thus, for MC-MP, the sizes of the small grains obtained are between 100-400 nm at a temperature of 1150ºC and reach sizes between 200-900 nm at a temperature of 1250ºC (Fig. 6 (a), (c)). Large grain sizes range from a maximum of 5.27 μm at 1150ºC to a maximum of 5.01 μm at 1250ºC. For the compositions in which a small amount of dopant (Pr) was added, the microstructure obtained was similar (Fig. 6 (b), (d)). Thus, at 1250ºC, for MC-MPPr, the maximum size obtained for large grains was 4.89 μm.

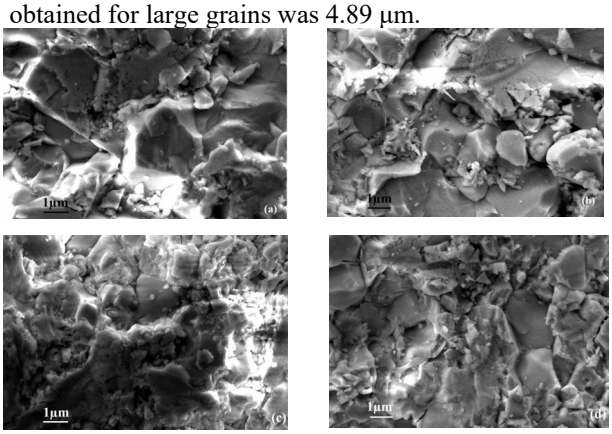

Fig. 6 SEM images of the samples sintered for 2 h at (i) 1150ºC (a) MC-MP, (b) MC-MPPr and (ii) 1250ºC (c) MC-MP (d) MC-MPPr

In Fig.7 are reported the SEM images of SPS sintered piezo materials. The SEM images mainly demonstrate submicron sized grains [24]. The granules have relatively narrow distributions of the graine size. The graine size also depends on the sintering temperature and composition. The average size of the granules decreases with the increase of the SPS sintering temperature from 1.9 μm to 1.6 μm for the SPS-MP composition, respectively from 1.8 μm to 1.5 μm for the SPS-MPPr composition.

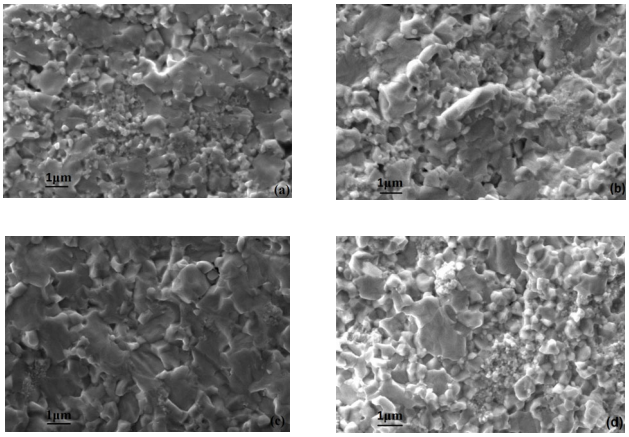

Fig. 7 SEM images of the samples sintered for 5' at (i) 850°C (a) SPS-MP, (b) SPS-MPPr and (ii) 950°C (c) SPS-MP (d) SPS-MPPr

Comparatively, the average size of the grains obtained by the modified conventional method is significantly larger. Also, the grain size distribution is wholly broader. In the case of compositions sintered by the conventional method, the densification mechanism is associated to the appearance of the liquid phase during sintering. This mechanism is not found during SPS sintering at temperatures up to 950°C [24].

Ferroelectric characteristics

In Fig. 8 - Fig. 11 are presented the hysteresis loops of unpoled piezo materials as a function of applied electric field.

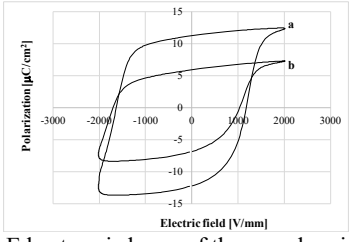

Fig. 8 P-E hysteresis loops of the samples sintered at 1150°C for 2 h (a) MC-MP, (b) MC-MPPr

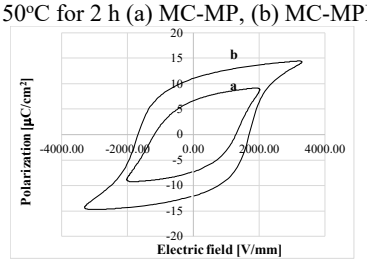

Fig. 9 P-E hysteresis loops of the samples sintered at 1250°C for 2 h (a) MC-MP, (b) MC-MPPr

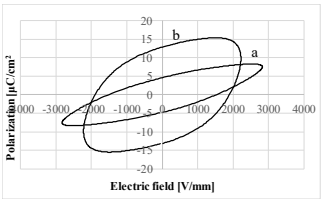

Fig. 10 SEM images of the samples sintered for 5'at 850°C (a) SPS-MP, (b) SPS-MPPr

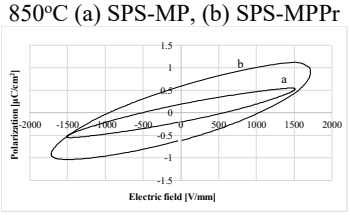

Fig. 11 SEM images of the samples sintered for 5'at 950°C (a) SPS-MP, (b) SPS-MPPr

It is observed that all the hysteresis loops are symmetric. The hysteresis loops obtained for the MC-MP and MC-MPPr sintered at 1150°C and 1250°C are typical for FE bulk materials. In the case of SPS sintering, the values obtained for the remnant polarization are very small and the coercive field obtained is relatively high (Table 4) [24].

The shape of the hysteresis loops depends on the nature of the phases obtained in the crystalline structure and it is influenced by the amount of the tetragonal phase.

Table 4: Remanent polarisation (P_r) and the coercitive field (E_c) values obtained for piezoelectric compositions function of sintering temperature

Samples	Temperature [°C]	E_c [V]	P_r [µC/cm²]
MC-MP	1150	1163	11.26
	1250	1714	16.33
MC-MPPr	1150	1022	5.93
	1250	1408	11.02
SPS-MP	850	1504	4.05
	950	552	0.36
SPS-MPPr	850	1892	10.93
	950	1020	1.11

The small values obtained for the residual polarization are associated with the submicron values obtained for the grain sizes [24].

Dielectric and piezoelectric properties

The values obtained for the dielectric and piezoelectric properties as a function of sintering are presented in Table 5. These values are dependent on grain size, crystal structure, sintering process and technological parameters. The relatively high values of the dielectric constants (dielectric permitivity (ε_r)

and dielectric losses (tan δ)) are due to the mobility of the domain walls [17].

Table 5: The dielectric and piezoelectric properties obtained for piezoelectric compositions function of sintering temperature

Samples	Temperature [°C]	ε_r	tgδ $*10^{-2}$	k_p
MC-MP	1150	960	0.86	0.27
	1250	1675	1.24	0.32
MC-MPPr	1150	1026	0.12	0.32
	1250	1953	1.43	0.43
SPS-MP	850	1386	0.84	0.20
	950	1365	2.01	0.24
SPS-MPPr	850	1356	4.66	0.21
	950	1677	2.54	0.27

The values obtained for the piezoelectric parameter (the planar coupling factor (k_p)) increases with increasing sintering temperature, the obtained microstructure being the determining factor. Through the SPS technique, at relatively low sintering temperatures, is possible to increase the level of densification as a result, one can improve the dielectric and piezoelectric properties.

5. Conclusions

In this paper B-oxide sintering process and Spark plasma Sintering (SPS) method were employed to develop $0.88Pb(Zr_{0.52}Ti_{0.48})O_3 - 0.12Pb(Mn_{1/3}Sb_{2/3})O_3$ – x at%Pr complex system. The aim of the research was the evaluation of the effect of sintering technique on the dielectric and ferroelectric properties of the piezoelectric materials. Based on the results obtained, the materials attained by the SPS technique reveals a lower remanent polarization and maximum strain, as well as a superior coercive field, compared to the those obtained employing the same composition produced by B-oxide method. Dense piezomaterials $0.88Pb(Zr_{0.52}Ti_{0.48})O_3 - 0.12Pb(Mn_{1/3}Sb_{2/3})O_3$ – x at% Pr was obtained by (i) SPS technique sintering for 5 min at lows temperature of 850°C and 950°C and (ii) conventional sintering method for 2 hours at 1150°C and 1250°C.

The microstructure, being dependent mainly on the grain size, can be considered as the main feature which influence and determine the differences between the values of the same property obtained by the two procedures. The obtained results indicate that the SPS technique can be considered an alternative technology for sintering piezoelectric materials belonging to complex systems based on PZT.

Acknowledgement

Authors are grateful for the support given by the project no. 133/23.09.2016, ID P_40_403, My SMIS code:105568 co-founded of the European Regional Development Funds through the 2014-2020 Operational Competitiveness Program-Subcontract no.133-D1 ICPE. The authors are especially grateful to their colleague Marinescu Virgil for his help for SEM micrographs, Patroi Delia for her help for XRD measurements and Pintea Jana for her help for electrical measurements.

References

[1] Lonkar, C. M. (2015), *Handbook of Nanoceramic and Nanocomposite Coatings and Materials, Chapter 25 Synthesis, Characterization, and Development of PZT-Based Composition for Power Harvesting and Sensors Application*, pp. 551–577.

[2] Hamzioui, L., Kahoul, F., Guemache, A., Aillerie, M. and Boutarfaia, A. (2021), Effect of Zr/Ti Ratio on Piezoelectric and Dielectric Properties of $0.1Pb[Fe_{1/2}Nb_{1/2}]O_3$-$0.9Pb[Zr_xTi_{(1-x)}]O_{30}$ Ceramics, *Transactions of the Indian Ceramic Society*, vol. 80(1), pp. 60-63.

[3] Miga, S., Molak, A. and Balin, K. (2020), The composition induced crossover in nonlinear dielectric response in $(1-x)$ $Pb(Zr_{0.70}Ti_{0.30})O_3$–x $BiMn_2O_5$ (x = 0, 0.02, 0.055, 0.11, 0.15, 0.22, and 1) ceramics, *J. Electroceram*, vol. 44, pp. 136–146.

[4] Yimnirun, R., Ananta, S. and Laoratanakul, P. (2004), Effects of $Pb(Mg_{1/3}Nb_{2/3})O_3$ mixed-oxide modification on dielectric properties of $Pb(Zr_{0.52}Ti_{0.48})O_3$ ceramics, *Materials Science and Engineering, B,* vol. 112(1), pp. 79–86.

[5] Du, G. et al. (2013), Large stable strain memory effect in poled Mn-doped $Pb(Mn_{1/3}Sb_{2/3})O_3$-$Pb(Zr,Ti)O_3$ ceramics, *Applied Physics Letters*, vol. 102(16), pp. 162907(1-4).

[6] Li, C.-L., Chou, C.-C., and Tsai, D.-S. (2005), Fabrication and electric properties of PZN-based ceramics using modified columbite method, *Journal of the European Ceramic Society*, vol. 25(12), pp. 2197–2200.

[7] Sun, H. J., Liu, X. F., Zhou, J., Xu, Q., Liu, H. X. and Chen, W. (2007), Structure, Electrical Properties of xPNN-(1-x)PMNS Pseudoquintnary System Piezoceramics, *Ferroelectrics*, vol. 358(1), pp. 49–53.

[8] Bochenek, D., and Niemiec, P. (2018), Microstructure and physical properties of the multicomponent PZT-type ceramics doped by calcium, sodium, bismuth and cadmium, *Applied Physics A*, vol. 124(11), pp. 775(1-7).

[9] Cheng, L.-Q. et al. (2018), Significantly improved piezoelectric performance of PZT-PMnN ceramics prepared by spark plasma sintering, *RSC Advances*, vol. 8(62), pp. 35594–35599.

[10] Seal, A., Mazumder, R., Sen, A. and Maiti, H. S. (2000), Fast firing of lead zirconate titanate ceramics at low temperature, *Materials Chemistry and Physics*, vol. 97(1), pp. 14–18.

[11] Corker, D. L., Whatmore, R. W., Ringgaard, E. and Wolny, W. W. (2000), Liquid-phase sintering of PZT ceramics, *Journal of the European Ceramic Society*, vol. 20(12), pp. 2039–2045.

[12] Hungría, T., Galy, J. and Castro, A. (2009), Spark Plasma Sintering as a Useful Technique to the Nanostructuration of Piezo-Ferroelectric Materials, *Advanced Engineering Materials*, vol. 11(8), pp. 615–631.

[13] Zhou, L., Zhao, Z., Zimmermann, A., Aldinger, F. and Nygren, M. (2004), Preparation and Properties of Lead Zirconate Stannate Titanate Sintered by Spark Plasma Sintering, *Journal of the American Ceramic Society*, vol. 87(4), pp. 606–611.

[14] Zhou, L., Rixecker, G., Aldinger, F., Zuo, R., and Zhao, Z. (2006), Electric Fatigue in Ferroelectric Lead Zirconate Stannate Titanate Ceramics Prepared by Spark Plasma Sintering, *Journal of the American Ceramic Society*, vol. 89(12), pp. 3868–3870.

[15] H. Vincent, X. Turrillas, I. Rasines: A novel structural type of hexagonal closest packing the ternary oxide, β-$MnSb_2O_6$. In: Materials Research Bulletin, 22(10), 1987, 1369–1379.

[16] Zhu, Z. G. , Li, G. R., Zheng, L. Y. and Yin, Q. R. (2005), Microstructure, domain morphology and piezoelectric properties of Si-doped $Pb(Mn_{1/3}Sb_{2/3})O_3$–$Pb(Zr,Ti)O_3$ systems, *Materials Science and Engineering, B*, vol. 119(1), pp. 46–50.

[17] Mudinepalli, V. and Leng, F. (2019), Dielectric and Ferroelectric Studies on High Dense $Pb(Zr_{0.52}Ti_{0.48})O_3$ Nanocrystalline Ceramics by High Energy Ball Milling and Spark Plasma Sintering, *Ceramics*, vol. 2(1), pp. 13–24.

[18] Randall, C. A., Kim, N., Kucera, J.-P., Cao, W. and Shrout, T. R. (2005), Intrinsic and Extrinsic Size Effects in Fine-Grained Morphotropic-Phase-Boundary Lead Zirconate Titanate Ceramics, *Journal of the American Ceramic Society*, vol. 81(3), pp. 677–688.

[19] Li, B., Zhu, Z., Li, G., Yin, Q. and Ding, A. (2004), Peculiar Hysteresis Loop of $Pb(Mn_{1/3}Nb_{2/3})O_3$–$Pb(Ti,Zr)O_3$ Ceramics, *Japanese Journal of Applied Physics*, vol. 43(4A), pp. 1458–1463.

[20] Dumitru, A. I. et al. (2020), Investigations on the Doping Effects on the Properties of Piezoelectric Ceramics, *Advanced Materials Research*, 1158, pp. 105-114.

[21] Wu, Y. J., Uekawa, N., Kakegawa, K. and Sasaki, Y. (2002), Compositional fluctuation and dielectric properties of $Pb(Zr_{0.3}Ti_{0.7})O_3$ ceramics prepared by spark plasma sintering, *Materials Letters*, vol. 57(3), pp. 771–775.

[22] Maiwa, H., Kimura, O., Shoji, K. and Ochiai, H. (2005), Low temperature sintering of PZT ceramics without additives via an ordinary ceramic route, *Journal of the European Ceramic Society*, vol. 25(12), pp. 2383–2385.

[23] Udomkan, N., Limsuwan, P. and Tunkasiri, T. (2007), Effect of rare-earth (RE = La, Nd, Ce AND Gd) doping on the piezoelectric of PZT(52:48) ceramics, *International Journal of Modern Physics, B,* vol. 21 (6), pp. 4549-4559.

[24] Takeuchi, T., Tabuchi, M., Kondoh, I., Tamari, N. and Kageyama, H. (2004), Synthesis of Dense Lead Titanate Ceramics with Submicrometer Grains by Spark Plasma Sintering, *Journal of the American Ceramic Society*, vol. 83(3), pp. 541–544.